

Nonuniform asymmetric exclusion process: Stationary densities and domain walls

Sudip Mukherjee^{1,2,*} and Abhik Basu^{2,†}

¹*Barasat Government College, 10, KNC Road, Gupta Colony, Barasat, Kolkata 700124, West Bengal, India*

²*Theory Division, Saha Institute of Nuclear Physics,
1/AF Bidhannagar, Calcutta 700064, West Bengal, India*

(Dated: October 31, 2024)

We explore the stationary densities in totally asymmetric exclusion processes (TASEP) with open boundary conditions and spatially inhomogeneous hopping rates. We calculate the steady state density profiles that characterise the associated phases. We show that in the contrast to the low and high density phases, the stationary density profile in the maximal current phase can be discontinuous, even when the space-dependent hopping rate is continuous. The phase diagrams in the plane of the control parameters show universal topology. The associated phase transitions are explored. We further investigate the domain walls, which are delocalised and calculate their envelopes, which reveal their dependence on the spatial nonuniformity of the hopping rates.

I. INTRODUCTION

The effects of quenched disorders on the macroscopic properties of equilibrium condensed matter systems have a long history of exploration within statistical mechanics models, giving good understanding of the ensuing equilibrium phenomena [1]. In contrast, the effects of disorders on dynamics and steady states of nonequilibrium models are far from being well-understood theoretically [2]. Lack of a general theoretical framework has prompted scientists to construct simple conceptual nonequilibrium models, where the effects of quenched disorders can be studied explicitly within simple approximations.

Totally asymmetric simple exclusion process (TASEP) is one of the best studied nonequilibrium model [3–5]. It was originally proposed as a simple model for protein synthesis in eukaryotic cells [7]. Later on, it has been reinvented as a paradigmatic one-dimensional (1D) model for nonequilibrium phase transitions in open systems [3]. A TASEP is defined as a one-dimensional lattice gas where particles are hopping stochastically in one direction subject to hard-core repulsion or *exclusion*; see, e.g., Ref. [8]. Subsequently, motivated by a variety of phenomena of biological and social origins, many generalisations of TASEP have been proposed and studied, which have revealed novel nonequilibrium phenomena and rich phase behaviours. For example, it has been found from a large number of studies that a TASEP lane coupled with weak particle nonconserving processes, be in exchange of particles with the embedding medium or with another lane executing diffusive dynamics or even another, second TASEP lane, with or without open boundaries, can display complex nonuniform steady states of various kinds [9–13, 16–18]. Similarly, the coupled dynamics of a TASEP lane diffusively exchanging particles with an embedding three-dimensional medium has been explored in Refs. [19–22], revealing the nontrivial effects

of three-dimensional diffusion on the stationary states in the TASEP lane.

A particularly interesting generalisation of TASEP involves a TASEP lane, open or closed with quenched disorder or defects. Two distinct kinds of disorders have been considered - particle-wise disorder, in which hopping rates may depend on the particle attempting to jump [23–25], or site-wise disorder, in which each site is associated with a quenched disordered hopping rate [14, 15, 26, 27, 29–31, 44]. Such site-wise disordered TASEP can be applied to wide-ranging phenomenologies, e.g., protein synthesis by messenger RNA with slow sites [32–36] and congestion in vehicular or pedestrian movements by road blocks - ever increasing phenomena in urban life [37]. In this work, we focus on a specific sub-class of a TASEP with quenched disorder hopping rates, in which the hopping rate varies *smoothly*, as opposed to randomly, with position along the TASEP lane [38–42, 48]. In Ref. [48], a TASEP in a ring geometry with smoothly varying hopping rate with finite number of discontinuities has been studied by mean-field theory (MFT) and Monte-Carlo simulations (MCS), revealing generic nonuniform steady states and domain walls. Analogous study for an open TASEP with smoothly varying hopping rates with one minimum has been done in Ref. [42], that reveals delocalised domain walls (DDW) of complex shapes and phase transitions marked by discontinuous changes in the average bulk densities between different phases. In this work, we generalise the studies in Ref. [42] by choosing spatially slowly varying hopping rates that either have isolated finite discontinuities or have more than one global minimum. We use MFT and MCS for our studies. We show how MFT together with physically intuitive arguments can be employed to capture the correct stationary density profiles, which agree with the MCS results. By systematically going beyond the MFT, we analytically construct the envelop of the DDW for our chosen hopping rate functions that generalises a DDW in the conventional open TASEP with uniform hopping rate. Finally we study the phase diagrams and associated phase transitions. We establish that phase diagrams have the same topology as the one for a uniform

*Electronic address: sudip.bat@gmail.com,aca.sudip@gmail.com

†Electronic address: abhik.123@gmail.com, abhik.basu@saha.ac.in

open TASEP, and may even be *exactly* identical to that for an open uniform TASEP, which can be achieved by tuning the space-dependence of the hopping rate. This rules out phase diagrams as reliable markers for different choices of the spatially nonuniform hopping rates. The remainder of this article is organised as follows. We lay out the construction of our model in Section II. Then in Section IV we construct the DDW profiles for various different space dependent hopping rates. Next in Section V, we obtain the phase diagrams and studied the associated phase transitions. Then in Section V A, we discuss our simulation algorithm. Finally, we summarise and discuss our results in Section VI.

II. MODEL

In this Section, we define our model. We consider an inhomogeneous TASEP in a 1D lattice with L sites, labelled by $i \in [1, L]$. As in the pure TASEP model [3–5], particles enter through the left end ($i = 1$) at rate α , hop unidirectionally from the left to the right, all subject to exclusion, and finally leave the system at site $i = L$ with a rate β . The hopping rate at site i depends upon i and is given by $q_i \leq 1$; see Fig. 1 for a schematic model diagram. The dynamics is subject to exclusion at all sites and every time step.

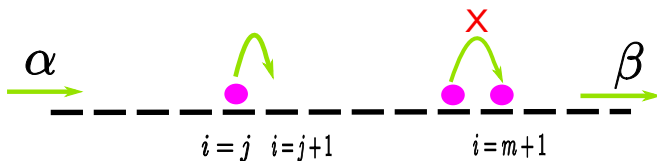


FIG. 1: Schematic model diagram. Broken line represents the TASEP lattice. Particles enter and exit at rates α and β , respectively, and hop from left to right, subject to exclusion. Hopping rate q_i at site i depends explicitly on the site index i .

Physically, we impose hard core repulsion between neighbouring particles, which prohibits multiple occupancy of sites in the model. The complete state space of our model then consists of 2^L configurations. The following elementary processes fully define the microscopic dynamical update rules of this model:

- (a) At any site $i = 1, \dots, L - 1$ a particle can jump to its neighbouring site $i + 1$ subject to exclusion with a rate $q_i \leq 1$.
- (b) At the site $i = 1$ a particle can enter the lattice with rate $\alpha q(1)$ provided it is unoccupied; and
- (c) At the site $i = N$ a particle can leave the lattice with rate $\beta q(L)$, if there is a particle there, i.e., when it is occupied.

In general, q_i is i -dependent, i.e., $q_i \neq q_j$ for $i \neq j$ in our model. Dynamical update rules (a)-(c) formally define an inhomogeneous TASEP with open boundary conditions. If all of $q_i = 1$ for all i identically, then

this model reduces to a pure TASEP with open boundary conditions and unit hopping rate [3]. In general, the form of the stationary densities should depend upon the specific choices of q_i [42]. We generalise the results of Ref. [42] and consider some specified choices of q_i that depends explicitly on i , and study their effects on the nonequilibrium steady states of the model below.

Before we embark on our studies below, we recall that the steady states of an open TASEP with α and β as the entry and exit rates, and a uniform hopping rate are characterised by the mean bulk density ρ_T : For $\alpha < \beta$ and $\alpha < 1/2$, one has $\rho_T = \alpha$ giving the low density (LD) phase, for $\beta < \alpha$ and $\beta < 1/2$, one has $\rho_T = 1 - \beta$ giving the high density (HD) phase, and for $\alpha, \beta > 1/2$, one has $\rho_T = 1/2$ giving the maximal current (MC) phase. This immediately gives the phase boundary in the $\alpha - \beta$ plane [3]. The principal aim of the present study is to find the phases, phase boundaries and the nature of the associated phase transitions, and the principles behind obtaining them when the hopping rate is not constant, but spatially smoothly varying. In Sec. III A, we construct the MFT for our model for specific choices of the space-dependent hopping rates.

III. STEADY STATE DENSITIES

Our aim is to study the stationary densities in the steady states and explore the domain walls, which are moving or *delocalised*, i.e., DDWs. For this purpose, we set up an MFT, amenable to analytical solutions for the steady state densities. We show how it can be applied to obtain unambiguous predictions on the steady state density profiles. By going beyond MFT, we further calculate the envelop of the DDWs analytically, which show that the DDW profiles actually depend rather *weakly* on the specific natures of space-dependent hopping rates. We supplement our analytical results by extensive MCS studies, which agree well with our analytical solutions.

A. Mean-field theory

We first consider the rate equations defined above for every site, which are *not* closed. The MFT approximation entails neglecting correlation effects and replacing the average of product of densities by the product of average of densities [43]. Although this is an approximation, this has worked with a good degree of accuracy in the original TASEP problem and also later in its many variants (see, e.g., Refs. [44–46]). The MFT dynamical equation for $n_i(t)$ reads

$$\frac{\partial n_i}{\partial t} = q_i n_{i-1} (1 - n_i) - q_{i+1} n_i (1 - n_{i+1}), \quad (1)$$

for a site i in the bulk. Our model exhibits *particle-hole symmetry* in the following sense: a jump of a particle to the right corresponds to a vacancy or hole movement by

one step to the left. Similarly, a particle entering the TASEP channel at the left boundary can be interpreted as a hole leaving it through the left boundary, and vice versa for the right boundary. Indeed, Eq. (1) is invariant under the transformation $n_i(t) \rightarrow 1 - n_{L-i}(t)$ together with $q_i \rightarrow q_{L-i}$ and $\alpha \rightarrow \beta$, which formally defines the *particle-hole symmetry* in this model [42, 46]. In our subsequent analysis below, for the ease of presentation of our results, we take a continuum limit with $\rho(x) \equiv \rho_i$, with $x = i/L$ becoming quasi-continuous in the limit $L \rightarrow \infty$ and $0 \leq x \leq 1$. In this parametrisation, the hopping rate function is given by $q(x)$, with $0 < q(x) \leq 1$. In this work, we consider few specific examples of $q(x)$, which vary *slowly* with x . We define a lattice constant $\varepsilon \equiv L_0/L$, where L_0 is the geometric length of the system, which has been set to unity without any loss of generality. In the limit $L \rightarrow \infty$, $\varepsilon \rightarrow 0$ is a small parameter in the problem. As shown in Refs. [42, 48], the general solution for the stationary density is

$$\rho(x) = \frac{1}{2} \left[1 \pm \sqrt{1 - \frac{4J}{q(x)}} \right], \quad (2)$$

where J is the stationary current, a constant throughout the system. In MFT, J depends on the specific phase the TASEP lane is in. We have

$$J_{LD} = q(0)\alpha(1 - \alpha), \quad (3)$$

$$J_{HD} = q(1)\beta(1 - \beta), \quad (4)$$

$$J_{MC} = \frac{q_{\min}}{4} \quad (5)$$

are, respectively, the currents in the LD, HD and MC phases of the TASEP lane. With these currents in (3)-(5), the stationary densities in the LD, HD and MC phases are [42]

$$\rho_{LD}(x) = \frac{1}{2} \left[1 - \sqrt{1 - \frac{4J}{q(x)}} \right] < 1/2, \quad J = J_{LD}, \quad (6)$$

$$\rho_{HD}(x) = \frac{1}{2} \left[1 + \sqrt{1 - \frac{4J}{q(x)}} \right] > 1/2, \quad J = J_{HD}, \quad (7)$$

$$\rho_{MC}(x) = \frac{1}{2} \left[1 - \sqrt{1 - \frac{q_{\min}}{q(x)}} \right] \equiv \rho_- < 1/2, \quad (8)$$

$$= \frac{1}{2} \left[1 + \sqrt{1 - \frac{q_{\min}}{q(x)}} \right] \equiv \rho_+ > 1/2. \quad (9)$$

Unsurprisingly, $\rho_{LD}(x), \rho_{HD}(x), \rho_{MC}(x)$ depend on the specific choices of the hopping rate function $q(x)$. Below we calculate the stationary densities for a few specific forms of $q(x)$. The choices for $q(x)$ made here either have more than one minimum or have one discontinuity. These choices complement and extend the studies in Ref. [42].

B. Case I

In Case I, we choose

$$q(x) = 1 - \left(x - \frac{1}{2} \right)^2. \quad (10)$$

In this case, $q(x)$ has a minimum of $3/4$ at $x = 0$ and $x = 1$, and has a maximum of 1 at $x = 1/2$. Thus $q(x)$ has two minima at the two end points of the TASEP lane and a single maximum in the bulk. The stationary densities $\rho_{LD}(x)$ and $\rho_{HD}(x)$ can be directly obtained from (6) and (7) with $q(x)$ as in (10) and $J = J_{LD}$ and $J = J_{HD}$, respectively. Our MFT results and the corresponding MCS results for $\rho_{LD}(x)$ and $\rho_{HD}(x)$ are shown in Fig. 2 (a) and Fig. 2 (b) respectively. We find good agreements between MFT and MCS results.

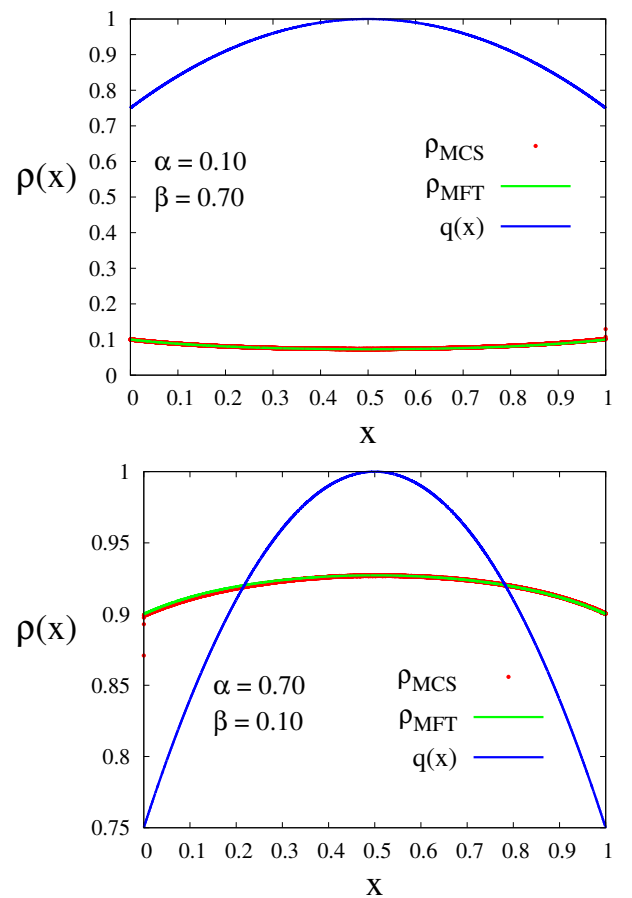


FIG. 2: Plots of the stationary densities as a function of x for $q(x)$ given by (10). (left) Density profile $\rho_{LD}(x)$ in the LD phase and (right) density profile $\rho_{HD}(x)$ in the HD phase. The blue curve denotes the hopping rate function $q(x)$. The MCS and MFT results on the density profiles are shown in points (green) and line (red). Good agreements between MFT and MCS results are found (see text).

We now study the MC phase stationary density $\rho_{MC}(x)$ that requires careful consideration. In the MC phase,

$J = q_{\min}/4$, which can be used in (8) or (9) to construct $\rho_{\text{MC}}(x)$. Thus the task now is to find out which part of the stationary MC phase density corresponds to $\rho_+(x)$ and which part $\rho_-(x)$.

To proceed, we imagine the TASEP lane to be composed of two TASEP lanes T_L and T_R connected serially at $x = x_0 = 1/2$, the location of the maximum of $q(x)$. In this representation, the hopping rate at the exit end of T_L , which is at $x = 1/2$, is unity, which is the hopping rate at the entry end of T_R . Notice that as $x \rightarrow 0, 1$, both $\rho_+(x), \rho_-(x) \rightarrow 1/2$. Since $\rho_{\text{MC}}(x)$ is either $\rho_-(x)$ or $\rho_+(x)$, this means $\rho_{\text{MC}}(x) = 1/2$ at both $x = 0, 1$ *definitely*, while $\rho_{\text{MC}}(x \rightarrow 1/2_{\pm})$ is *definitely not* $1/2$, since neither of $\rho_+(x), \rho_-(x)$ is $1/2$ there. Let us first focus on T_L . It has a stationary density of $1/2$ at $x = 0$, its entry end, and a different value at $x = 1/2$, its exit end. Thus, the density profile in T_L resembles a stationary density found on the LD-MC phase boundary, in which $J = J_{\max} = q_{\min}/4$, and has a density $1/2$ at the entry end. This arguments suggests that between $x = 0$ and $x = 1/2$, $\rho_{\text{MC}}(x) = \rho_-(x)$ in the bulk, since $\rho_i(x)$ has a density of $1/2$ at its entry end and has a value different from $1/2$ at its exit end. We next consider T_R . The stationary density on T_R *definitely* has a value $1/2$ at $x = 1$, its exit end, but has a value *different from* $1/2$ at $x = 1/2$, its entry end. Thus, the steady state density on T_R resembles the stationary density on the HD-MC phase boundary, in which $J = J_{\max} = q_{\min}/4$, and has a density $1/2$ at its exit end. This arguments suggests that between $x = 1/2$ and $x = 1$, $\rho_{\text{MC}}(x) = \rho_+(x)$ in the bulk. We thus arrive at the following MFT solution for $\rho_{\text{MC}}(x)$:

$$\begin{aligned} \rho_{\text{MC}}(x) &= \rho_-(x), \quad 0 \leq x \leq 1/2, \\ &= \rho_+(x), \quad 1/2 \leq x \leq 1. \end{aligned} \quad (11)$$

We have plotted (11) in Fig. 3. We find excellent agreement with the corresponding MCS result. Notice that in this case the average MC phase density

$$\bar{\rho}_{\text{MC}} \equiv \int_0^1 \rho_{\text{MC}}(x) dx = \frac{1}{2}, \quad (12)$$

same as that for the MC in a uniform open TASEP. There is a however a fundamental distinction between the two. In a uniform open TASEP, $\rho_{\text{MC}}(x) = 1/2$ *everywhere* in the TASEP lane (excluding the boundary layers). In contrast, in Case I here, $\rho_{\text{MC}}(x) = 1/2$ *only* for $x \rightarrow 0, 1$. Everywhere else in the bulk, it is *different* from $1/2$.

C. Case II

In Case II, we consider

$$\begin{aligned} q(x) &= \frac{1}{1+2x}, \quad 0 \leq x \leq 1/2, \\ &= \frac{1}{2x}, \quad 1/2 \leq x \leq 1. \end{aligned} \quad (13)$$

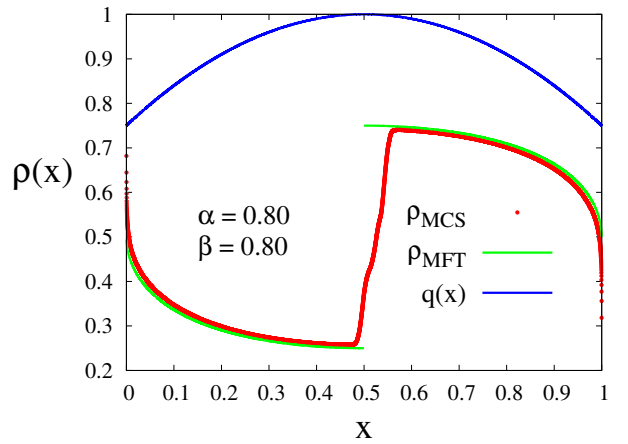


FIG. 3: Plot of the stationary density $\rho_{\text{MC}}(x)$ in the MC phase for $q(x)$ given by (10). The blue curve denotes the hopping rate function $q(x)$. The MCS and MFT results on the density profiles are shown in points (green) and line (red). Good agreements between MFT and MCS results are found (see text).

Thus $q(x)$ is discontinuous at $x = 1/2$. It has a maximum value of unity at $x = 0$ and $x \rightarrow 1/2_+$, and has minimum value of $1/2$ at $x \rightarrow 1/2_-$ and $x = 1$. Thus it has two maxima and two minima. Stationary densities $\rho_{\text{LD}}(x)$ and $\rho_{\text{HD}}(x)$ can be straightforwardly obtained from (6) and (7) above together with $q(x)$ given in (13). Unsurprisingly, both $\rho_{\text{LD}}(x) < 1/2$ and $\rho_{\text{HD}}(x) > 1/2$ have discontinuities at $x = 1/2$, reflecting the discontinuity of $q(x)$ at that point. Our MFT results for $\rho_{\text{LD}}(x)$ and $\rho_{\text{HD}}(x)$ superposed with the corresponding MCS results are shown in Fig. 4(a) and Fig. 4(b) respectively. We find excellent agreements between the two.

We now focus on $\rho_{\text{MC}}(x)$, the stationary MC phase density. As in the previous case, both $\rho_+(x)$ and $\rho_-(x)$ with $q(x)$ in (13) have a steady current $J = J_{\max} = q_{\min}/4$. We must decide whether $\rho_+(x)$ or $\rho_-(x)$ or both should be used to construct $\rho_{\text{MC}}(x)$ in MFT. We proceed as in the previous case. We imagine the TASEP lane to be composed of two segments T_L ($0 \leq x \leq 1/2$) and T_R ($1/2 < x < 1$) connected serially at $x = 1/2$. In the present case, we have $\rho_+(x \rightarrow 1/2_-) = 1/2 = \rho_-(x \rightarrow 1/2_-)$ and $\rho_+(x \rightarrow 1_-) = 1/2 = \rho_-(x \rightarrow 1_-)$. Let us focus on T_L first. We use arguments similar to the previous example. On T_L , we must have $\rho_{\text{MC}}(x \rightarrow 1/2_-) = 1/2$ as *both* $\rho_+(x)$ and $\rho_-(x)$ approach $1/2$ at point, whereas $\rho_{\text{MC}}(x)$ *must be different* from $1/2$ at $x = 0$, since *both* $\rho_+(x)$ and $\rho_-(x)$ are *different* from $1/2$ at that point. Thus, on T_L we have a stationary density that is $1/2$ at $x \rightarrow 1/2_-$, the exit end, but is different from $1/2$ at $x = 0$, its entry end, and hence resembles the stationary density profile on the HD-MC boundary of an open TASEP. We thus expect $\rho_+(x)$ to be the stationary density on the TASEP lane in the range $0 \leq x \leq 1/2$. We now consider T_R . We have the stationary density $1/2$ at $x = 1$, since *both* $\rho_+(x)$ and $\rho_-(x)$ approach $1/2$ at point,

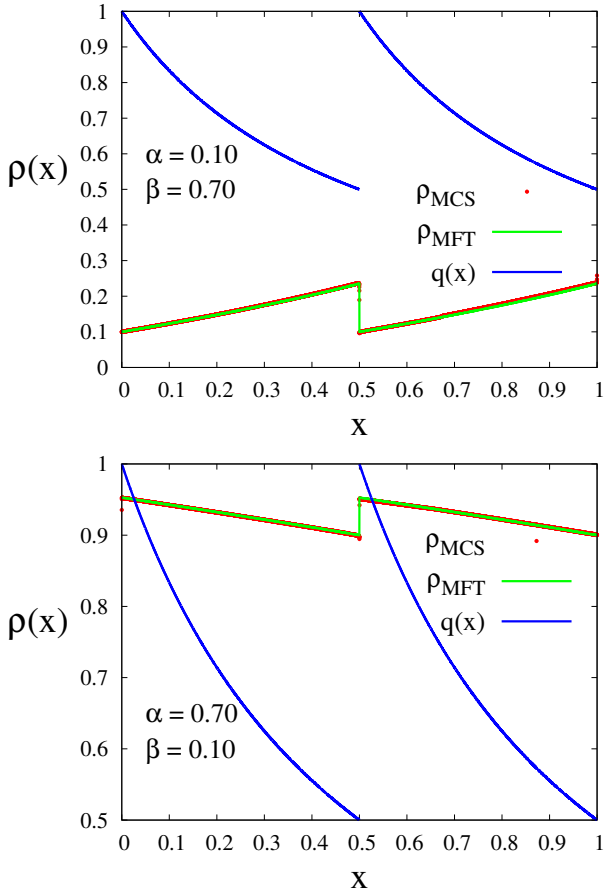


FIG. 4: Plots of the stationary densities as a function of x for $q(x)$ given by (13). (left) Density profile $\rho_{LD}(x)$ in the LD phase and (right) density profile $\rho_{HD}(x)$ in the HD phase. The blue curve denotes the hopping rate function $q(x)$. The MCS and MFT results on the density profiles are shown in points (green) and line (red). Good agreements between MFT and MCS results are found (see text).

whereas $\rho_{MC}(x)$ must be different from $1/2$ at $x \rightarrow 1/2_+$, since both $\rho_+(x)$ and $\rho_-(x)$ are different from $1/2$ at that point. Thus, the steady state density profile on T_R resembles that on the HD-MC boundary. Hence, we expect $\rho_+(x, J = q_{\min}/4)$ to be the stationary density on the TASEP lane in the range $1/2 \leq x \leq 1$. We thus conclude that

$$\rho_{MC}(x) = \rho_+(x) \quad (14)$$

in the entire TASEP lane. Our MFT agrees well with the corresponding MCS result; see Fig. 5. Since $\rho_+(x) > 1/2$ everywhere in the TASEP lane except at $x \rightarrow 1/2_-$ and $x = 1$, we must have $\bar{\rho}_{MC} > 1/2$ in contrast to a uniform open TASEP.

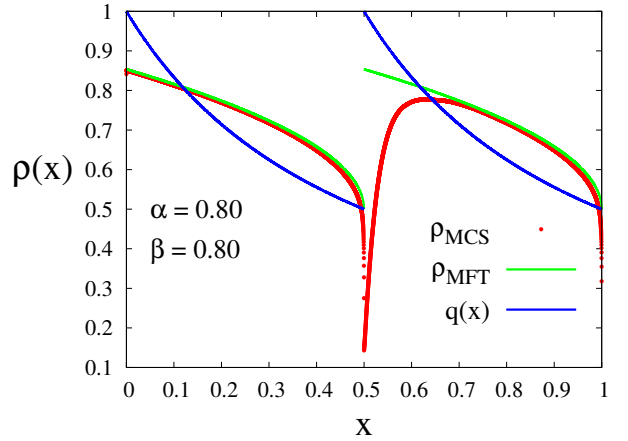


FIG. 5: Plot of the stationary density $\rho_{MC}(x)$ in the MC phase for $q(x)$ given by (13). The blue curve denotes the hopping rate function $q(x)$. The MCS and MFT results on the density profiles are shown in points (green) and line (red). Good agreements between MFT and MCS results are found (see text).

D. Case III

We now consider

$$\begin{aligned} q(x) &= \frac{1}{2-2x}, 0 \leq x \leq 1/2, \\ &= \frac{1}{3-2x}, 1/2 \leq x \leq 1. \end{aligned} \quad (15)$$

This is in fact the mirror image of $q(x)$ in (13) about $x = 1/2$. Thus $q(x)$ is discontinuous at $x = 1/2$. It has two minima of value $1/2$ at $x = 0$ and $x \rightarrow 1/2_+$, and two maxima at $x \rightarrow 1/2_-$ and $x = 1$. Stationary densities $\rho_{LD}(x)$ and $\rho_{HD}(x)$ can be straightforwardly obtained from (6) and (7) above together with $q(x)$ given in (15). Unsurprisingly, both $\rho_{LD}(x) < 1/2$ and $\rho_{HD}(x) > 1/2$ have discontinuities at $x = 1/2$, reflecting the discontinuity of $q(x)$ at that point. Our MFT results for $\rho_{LD}(x)$ and $\rho_{HD}(x)$ superposed with the corresponding MCS results are shown in Fig. 6(a) and Fig. 6(b) respectively. We find excellent agreements between the two.

We now focus on $\rho_{MC}(x)$, the stationary MC phase density. As in the previous case, both $\rho_+(x)$ and $\rho_-(x)$ with $q(x)$ in (15) have a steady current $J = J_{\max} = q_{\min}/4$. We thus need to decide whether $\rho_+(x)$ or $\rho_-(x)$ or both should be used to construct $\rho_{MC}(x)$ in MFT. We proceed as in the previous case. Once again we imagine the TASEP lane to be composed of two segments T_L ($0 \leq x \leq 1/2$) and T_R ($1/2 < x < 1$) connected serially at $x = 1/2$. In the present case, we have $\rho_+(x \rightarrow 0) = 1/2 = \rho_-(x \rightarrow 0)$ and $\rho_+(x \rightarrow 1/2_+) = 1/2 = \rho_-(x \rightarrow 1/2_+)$. Let us focus on T_L first. We use arguments similar to the previous example. On T_L , we must have $\rho_{MC}(x \rightarrow 0) = 1/2$ as both $\rho_+(x)$ and $\rho_-(x)$ approach $1/2$ at point, whereas $\rho_{MC}(x)$ must be different from $1/2$ at $x = 1/2_-$, since both $\rho_+(x)$ and $\rho_-(x)$ are different from $1/2$ at

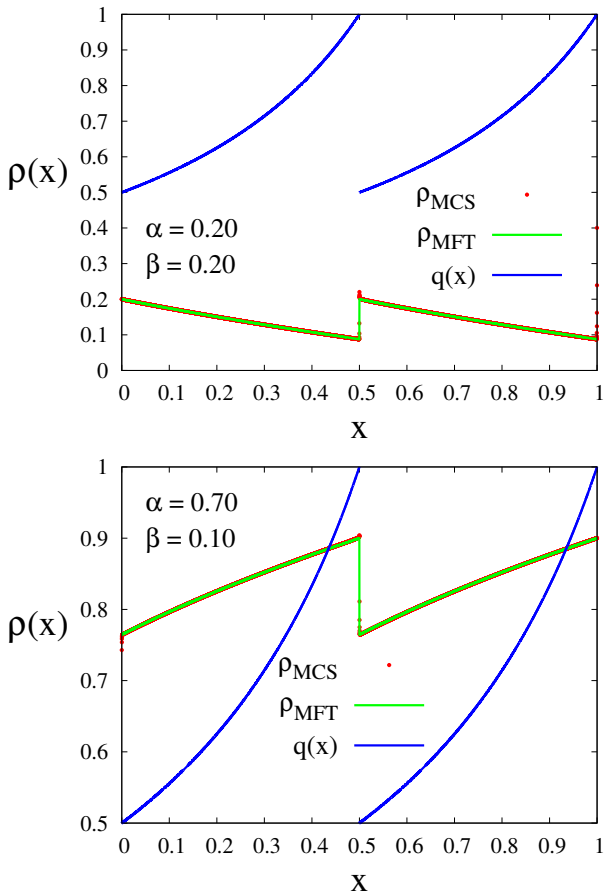


FIG. 6: Plots of the stationary densities as a function of x for $q(x)$ given by (15). (left) Density profile $\rho_{LD}(x)$ in the LD phase and (right) density profile $\rho_{HD}(x)$ in the HD phase. The blue curve denotes the hopping rate function $q(x)$. The MCS and MFT results on the density profiles are shown in points (green) and line (red). Good agreements between MFT and MCS results are found (see text).

that point. Thus, on T_L we have a stationary density that is $1/2$ at $x \rightarrow 0$, the entry end, but is different from $1/2$ at $x = 1/2$, its exit end, and hence resembles the stationary density profile on the LD-MC boundary of an open TASEP. We thus expect $\rho_-(x, J = q_{\min}/4)$ to be the stationary density on the TASEP lane in the range $0 \leq x \leq 1/2$. We now consider T_R . We have the stationary density $1/2$ at $x = 1/2_+$, since *both* $\rho_+(x)$ and $\rho_-(x)$ approach $1/2$ at point, whereas $\rho_{MC}(x)$ *must be different* from $1/2$ at $x \rightarrow 1$, since *both* $\rho_+(x)$ and $\rho_-(x)$ are *different* from $1/2$ at that point. Thus, the steady state density profile on T_R resembles that on the LD-MC boundary. Hence, we expect $\rho_-(x, J = q_{\min}/4)$ to be the stationary density on the TASEP lane in the range $1/2 \leq x \leq 1$. We thus conclude that

$$\rho_{MC}(x) = \rho_-(x, J = q_{\min}/4) \quad (16)$$

in the entire TASEP lane. Our MFT agrees well with the corresponding MCS result; see Fig. 7.

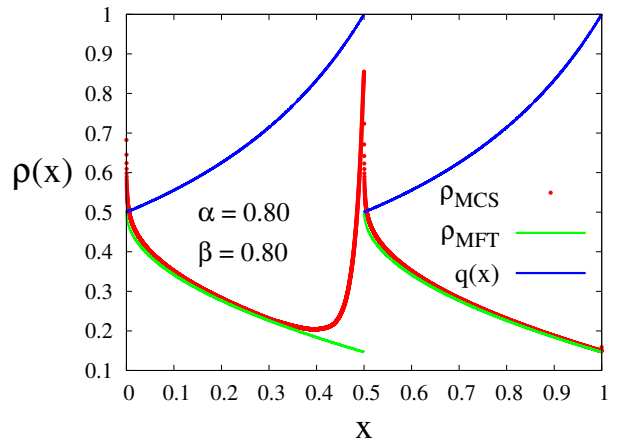


FIG. 7: Plot of the stationary density $\rho_{MC}(x)$ in the MC phase for $q(x)$ given by (15). The blue curve denotes the hopping rate function $q(x)$. The MCS and MFT results on the density profiles are shown in points (green) and line (red). Good agreements between MFT and MCS results are found (see text).

Since $\rho_-(x) < 1/2$ *everywhere* in the TASEP lane except at $x \rightarrow 0$ and $x \rightarrow 1/2_+$, we must have $\bar{\rho}_{MC} < 1/2$ in contrast to a uniform open TASEP.

IV. DELOCALISED DOMAIN WALLS

We now consider a DDW in a TASEP lane with an inhomogeneous hopping rate function $q(x)$. A DDW in an open TASEP with uniform hopping rate is formed on the line $\alpha = \beta < 1/2$, which is the phase boundary between the LD and HD phase. In an inhomogeneous open TASEP this condition is generalised to

$$J_{in} \equiv q(0)\alpha(1-\alpha) \equiv J_{out} = q(1)\beta(1-\beta) < J_{MC} \equiv \frac{q_{\min}}{4}. \quad (17)$$

Notice that the coexistence line takes the usual form $\alpha = \beta$ (as in an open TASEP), so long as $q(0) = q(1)$, *even if* $q(x)$ in general is *nonuniform*. This gives the coexistence line, which is the phase boundary between the LD and HD phases, in an open TASEP with nonuniform hopping rates. In an open uniform TASEP, a DDW profile connects $\rho_{LD} = \alpha$ at $x = 0$ and $\rho_{HD} = 1 - \beta$ at $x = 1$ with $\alpha = \beta$ through a straight line, which is the coexistence line. In the present study, with space dependent $q(x)$, the DDW profile still connects $\rho_{LD}(x = 0) = \alpha$ and $\rho_{HD}(x = 1) = 1 - \beta$ (however $\alpha \neq \beta$ in general), but *not* through a straight line anymore. Our aim in this Section is to calculate the equation for this line.

As in a uniform open TASEP, a DDW in the present model is actually the envelop of a series of LDWs. Let x_w be the position of an LDW with height $\Delta(x_w)$. Unlike in an open uniform TASEP, Δ now depends explicitly on x_w , due to the spatially nonuniform hopping rates.

If we increase the number of particle in the TASEP lane by one, i.e., if one particle enters the TASEP lane through the left (entry) end, the LDW position x_w shifts by an amount $-1/[L\Delta(x_w)]$ (to the left) [47, 48]. Similarly, when one particle leaves the TASEP lane through the right (exit) end, the LDW shifts by an amount $1/[L\Delta(x_w)]$ to the right. Thus there are two basic microscopic processes, which alter the particle number of the TASEP lane and make the LDW shift position:

(i) One particle entering through the left boundary of the TASEP lane. The corresponding transition rate is given by

$$W_L = q(0)\alpha(1 - \alpha), \delta x_w = -L^{-1}\Delta^{-1}.$$

(ii) One particle exiting through the right boundary of the TASEP lane. The corresponding transition rate is given by

$$W_R = q(1)\beta(1 - \beta), \delta x_w = +L^{-1}\Delta^{-1}.$$

Note that W_L and W_R are just the entry and exit currents, respectively.

Let $P(x_w, t)$ be the probability of finding a DW at x_w in the TASEP lane at time t . The master equation that P satisfies has the general form

$$\begin{aligned} \frac{\partial P}{\partial t} &= \sum_{\delta x_w} P(x_w + \delta x_w, t)W(x_w + \delta x_w \rightarrow x_w) \\ &- \sum_{\delta x_w} P(x_w, t)W(x_w \rightarrow x_w + \delta x_w). \end{aligned} \quad (18)$$

By using the different transition rates defined above, we can calculate the average shift or the expectation value of the change δx_w , given by

$$\begin{aligned} \langle \delta x_w \rangle &\equiv \sum [\text{signed increment } \delta x_w \times \text{transition rates}] \\ &= \frac{1}{L\Delta(x_w)} [q(1)\beta(1 - \beta) - q(0)\alpha(1 - \alpha)] = 0 \end{aligned} \quad (19)$$

at the delocalisation transition. This gives

$$q(1)\beta(1 - \beta) = q(0)\alpha(1 - \alpha) \quad (20)$$

as the condition for delocalisation that in simple terms just means ‘‘incoming current = outgoing current’’, and generalises the well-known $\alpha = \beta$ condition for a DDW in an open uniform TASEP [43], as mentioned above. In general, with $q(0) \neq q(1)$, the delocalisation line (20) is a curved line. If \bar{x}_w is the mean position of the DDW, then $\delta x_w \equiv x_w - \bar{x}_w$ is the fluctuation around the mean. We now expand the master equation (18) around the mean \bar{x}_w up to second order in δx_w . We obtain

$$\begin{aligned} \frac{\partial P}{\partial t} &= \sum_{\delta x_w} P(x_w + \delta x_w, t)W(x_w + \delta x_w \rightarrow x_w) - \sum_{\delta x_w} P(x_w, t)W(x_w \rightarrow x_w + \delta x_w) \\ &= \sum_{\delta x_w} P(x_w, t)W(x_w \rightarrow x_w + \delta x_w) - \frac{\partial}{\partial x_w} \sum_{\delta x_w} [\delta x_w P(x_w, t)W(x_w \rightarrow x_w + \delta x_w)] \\ &+ \frac{1}{2} \partial^2 \sum_{\delta x_w} [\delta x_w^2 P(x_w, t)W(x_w \rightarrow x_w + \delta x_w)] - \sum_{\delta x_w} P(x_w, t)W(x_w \rightarrow x_w + \delta x_w) \\ &= -\frac{\partial}{\partial y} [a(y)P(y, t)] + \frac{1}{2} \frac{\partial^2}{\partial y^2} [B(y)P(y, t)]. \end{aligned} \quad (21)$$

Here $y \equiv x_w$ and

$$\begin{aligned} a(x_w) &= \sum_{\delta x_w} \delta x_w W(x_w \rightarrow x_w + \delta x_w) \\ &= \frac{1}{L\Delta(x_w)} [-q(0)\alpha(1 - \alpha) + q(1)\beta(1 - \beta)], \quad (22) \\ B(x_w) &= \sum_{\delta x_w} \delta x_w^2 W(x_w \rightarrow x_w + \delta x_w) \\ &= \frac{1}{L^2\Delta^2(x_w)} [q(0)\alpha(1 - \alpha) + q(1)\beta(1 - \beta)] > 0. \end{aligned} \quad (23)$$

Equation (21) is the Fokker-Planck equation for the DW position x_w . The first terms in the last line of (21) is the drift term, and the last term is the diffusion term. At the delocalisation transition $a(x_w) = 0$. Thus the drift term vanishes, giving

$$\frac{\partial P}{\partial t} = \frac{\partial^2}{\partial y^2} [B(y)P(y)] = 0, \quad (24)$$

which is the Fokker-Planck equation at the delocalisation transition. Treating $P(y)$ as a conserved diffusing density, Eq. (24) is reminiscent of the conserved model

B relaxational dynamics [49] of a noninteracting density (an ideal gas), fluctuating about its mean, with an effective space-dependent inverse susceptibility or inverse compressibility $\chi^{-1}(y) \equiv B(y)$. Equation (24) allows us to identify a “current” $j(y) = \frac{\partial}{\partial y}[B(y)P(y)]$.

Now setting $\partial_t P = 0$ in the steady state, we find

$$\frac{\partial^2}{\partial y^2}[B(y)P(y)] = 0, \quad (25)$$

at the delocalisation transition.

Since the domain wall executes equilibrium dynamics [48, 50] we set $j(y) = 0$. Solving this, we find

$$P(y) = \frac{C}{B(y)}, \quad (26)$$

where C is a constant of integration. Recall that $y = x_w$, the position of the domain wall, and

$$\Delta(x_w) \equiv \rho_{\text{HD}}(x_w) - \rho_{\text{LD}}(x_w), \quad (27)$$

is the height of the domain wall, which is *also space-dependent* here. In an open TASEP with uniform hopping rates, Δ is a constant, independent of x_w . In contrast, both ρ_{HD} and ρ_{LD} in the present problem are in general nonuniform, depending explicitly on x_w . From (26), we find

$$P(x) \propto B(x)^{-2} \propto [\rho_{\text{HD}}(x) - \rho_{\text{LD}}(x)]^2, \quad (28)$$

depends on the coordinate x is maximum (minimum), where the height difference between the HD and LD solutions are maximum (minimum). Using our conceptual mapping to an ideal gas with a nonuniform compressibility, we note that $P(x)$, a measure of the local density fluctuations in this intuitive picture in terms of a conserved diffusing density, rises in regions with *higher* compressibility (or lower $B(x)$). This is easy to understand: in regions with higher compressibility, the free energy cost of higher fluctuations is smaller, letting the gas fluctuate more. In the domain wall picture (as here), a larger $P(x)$ in a region implies, larger probability of finding the DW in that region.

We now calculate the density profile of the DDW $\rho_{\text{DDW}}(x)$ starting by relating it to $P(x)$. As argued in Ref. [48], we must have

$$\frac{dP}{dx} = DP(x), \quad (29)$$

where $D > 0$ is a constant. Solving (29), we get

$$\rho(x) = D \int dx P(x) + B = A \int dx [\rho_{\text{HD}}(x) - \rho_{\text{LD}}(x)]^2 + B. \quad (30)$$

Constants A and B may be fixed by using the boundary conditions $\rho_{\text{DDW}}(0) = \alpha$, $\rho_{\text{DDW}}(1) = 1 - \beta$. Now, use (6) and (7) respectively for $\rho_{\text{LD}}(x)$ and $\rho_{\text{HD}}(x)$. For a DDW,

$$J_{\text{LD}} = q(0)\alpha(1 - \alpha) = J_{\text{HD}} = q(1)\beta(1 - \beta) = J_{\text{DDW}}. \quad (31)$$

We then find

$$\Delta(x) \equiv \rho_{\text{HD}}(x) - \rho_{\text{LD}}(x) = \sqrt{1 - \frac{4J_{\text{DDW}}}{q(x)}}, \quad (32)$$

which is the domain wall “height” at x . Notice that in the equivalent picture in terms of an ideal gas, its compressibility $\propto \Delta^2$ locally.

We now apply the above theory to several specific examples delineated by different forms for the hopping rate function $q(x)$ and calculate the shapes of the DDWs on the respective coexistence lines.

(i) We first consider

$$q(x) = \frac{1}{1+x}, \quad (33)$$

such that at $x = 0$, $q(0) = 1$ (maximum) and at $x = 1$, $q(1) = 1/2$ (minimum). The equation for the coexistence line in the present case is obtained from (17) and reads

$$\beta = \frac{1}{2} \left[1 - \sqrt{1 - 8\alpha(1 - \alpha)} \right]. \quad (34)$$

By using (30), we then get the stationary density on the coexistence line (34):

$$\rho_{\text{DDW}}(x) = Ax(1 - 4J_{\text{DDW}}) - 2AJ_{\text{DDW}}x^2 + B. \quad (35)$$

Using the boundary conditions $\rho_{\text{DDW}}(x = 0) = \alpha$ and $\rho_{\text{DDW}}(x = 1) = 1 - \beta$, we find

$$A = \frac{1 - \beta - \alpha}{1 - 6J_{\text{DDW}}}, \quad B = \alpha, \quad (36)$$

giving

$$\rho_{\text{DDW}}(x) = \frac{1 - \beta - \alpha}{1 - 6J_{\text{DDW}}} [x(1 - 4J_{\text{DDW}}) - 2J_{\text{DDW}}x^2] + \alpha. \quad (37)$$

The DDW profile (37) has been plotted (red line) in Fig. 8(a) together with the corresponding MCS result (black dots). Good agreements between the two is visible. We have also plotted $P(x)$ or $\Delta(x)$ from our MFT; see Fig. 8(b).

(ii) Next, we consider

$$q(x) = \frac{1}{2-x}. \quad (38)$$

Thus, at $x = 0$, $q(0) = 1/2$ (minimum) and at $x = 1$, $q(1) = 1$ (maximum). The equation for the coexistence line in the present case is obtained from (17) and reads

$$\alpha = \frac{1}{2} \left[1 - \sqrt{1 - 8\alpha(1 - \alpha)} \right]. \quad (39)$$

By using the boundary conditions $\rho_{\text{DDW}}(x = 0) = \alpha$ and $\rho_{\text{DDW}}(x = 1) = 1 - \beta$, we get

$$\rho_{\text{DDW}}(x) = \frac{1 - \alpha - \beta}{1 - 6J_{\text{DDW}}} [x(1 - 8J_{\text{DDW}}) + 2J_{\text{DDW}}x^2] + \alpha. \quad (40)$$

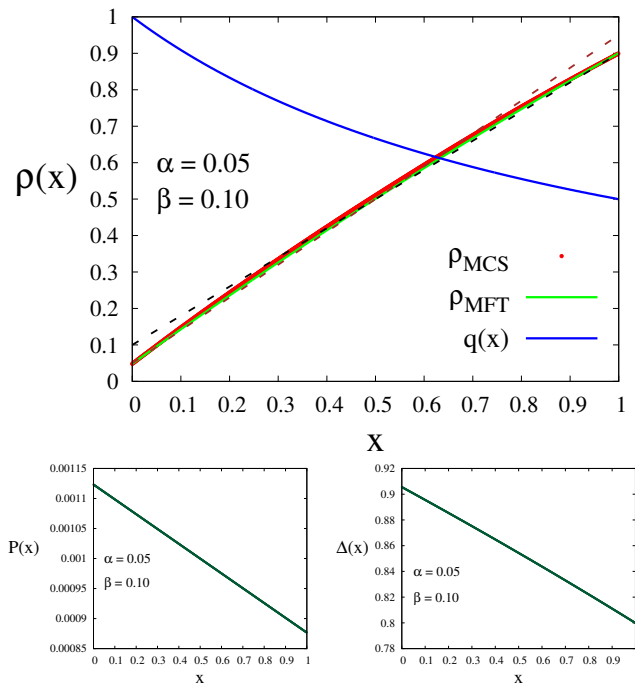


FIG. 8: (top) Density profile (37) for $\rho_{\text{DDW}}(x)$ on the coexistence line (34) with $q(x)$ as given in (33) and $\alpha = 0.05, \beta = 0.1$. Both MFT (green line) and MCS (red dots, system size $L = 1000$) are shown, which agree well with each other. The broken lines correspond to $\alpha = \beta = 0.05$ and $\alpha = \beta = 0.1$, which would have been the DDW profile in an open, uniform TASEP. (bottom) Plots of the corresponding local probability $P(x)$ (left) and domain wall height $\Delta(x)$ (right) are shown. Both are space-dependent. see text.

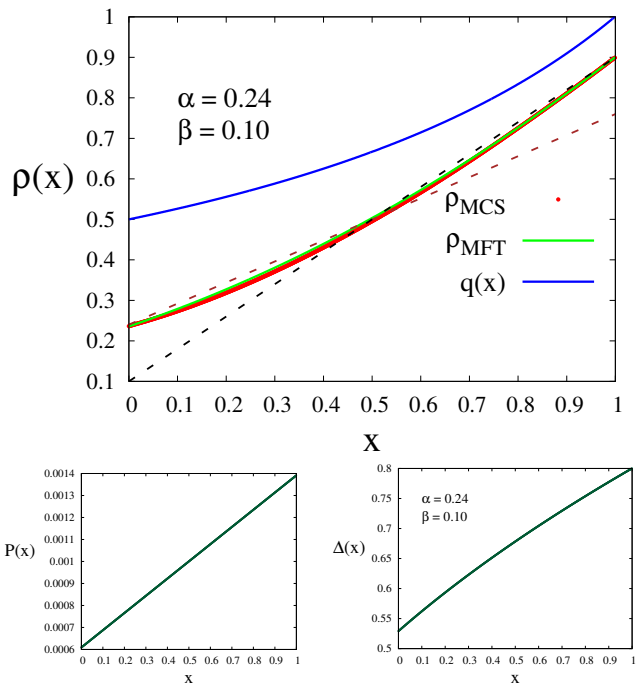


FIG. 9: (top) Density profile (37) for $\rho_{\text{DDW}}(x)$ on the coexistence line (39) with $q(x)$ as given in (38) and $\alpha = 0.24, \beta = 0.1$. Both MFT (green line) and MCS (red dots, system size $L = 1000$) are shown, which agree well with each other. The broken lines correspond to $\alpha = \beta = 0.24$ and $\alpha = \beta = 0.1$, which would have been the DDW profile in an open, uniform TASEP. (b) (bottom) Plots of the corresponding local probability $P(x)$ (left) and domain wall height $\Delta(x)$ (right) are shown. Both are space-dependent. see text.

We have presented this above DDW profile (40) along with the corresponding MCS results in Fig. 9(a), showing good agreements between the two. We have also plotted $P(x)$ or $\Delta(x)$ from our MFT; see Fig. 9(b).

(iii) So far we have studied the DDW profiles with $q(x)$, which are *continuous*, and also *smooth*, i.e., $dq(x)/dx$ is also continuous. We now consider a case, where $q(x)$ is continuous, but not smooth, i.e., $dq(x)/dx$ has a finite discontinuity in the bulk. For that, we consider a hopping rate function

$$q(x) = \frac{1}{1+ax}, \quad 0 \leq x \leq x_0, \\ = \frac{1}{3-bx}, \quad x_0 \leq x \leq 1. \quad (41)$$

Here, a, b are positive constants. What is x_0 ? It is determined by the imposed condition $q(x \rightarrow x_{0+}) = q(x \rightarrow x_{0-})$. This gives

$$x_0 = \frac{2}{a+b}. \quad (42)$$

Given the form of $q(x)$ in (41), we find that if $x_0 = 1/2$ along with $a = b = 2$, $q(x)$ is symmetric about $x = 1/2$,

the midpoint of the system; else, for any $x_0 \neq 1/2$, it is asymmetric. Clearly, dq/dx has a finite discontinuity at $x = x_0$. Since (29) is valid in the full domain of $x \in [0, 1]$, we write the general solution to (29) for $q(x)$ as in (41) as

$$\rho_{\text{DDW}}(x) = A \int dx [\rho_{\text{HD}}(x) - \rho_{\text{LD}}(x)]^2 + B_1, \quad 0 \leq x \leq x_0 \\ = A \int dx [\rho_{\text{HD}}(x) - \rho_{\text{LD}}(x)]^2 + B_2, \quad x_0 \leq x \leq 1, \quad (43)$$

which automatically ensures that $d\rho_{\text{DDW}}/dx$ follows the same equation in the entire domain $x \in [0, 1]$. Since $q(x)$ is continuous everywhere, $\rho_{\text{DDW}}(x)$ must also be continuous everywhere. Constants A, B_1, B_2 may be evaluated from the boundary conditions on $\rho_{\text{DDW}}(0), \rho_{\text{DDW}}(1)$ and the condition $\rho_{\text{DDW}}(x \rightarrow x_{0-}) = \rho_{\text{DDW}}(x \rightarrow x_{0+})$. We now use (41) to obtain the corresponding $\rho_{\text{DDW}}(x)$, which generally reads

$$\rho_{\text{DDW}}(x) = A(1 - 4J_{\text{DDW}})x - 2AJ_{\text{DDW}}ax^2 + B_1, \\ = A(1 - 12J_{\text{DDW}})x + 2AJ_{\text{DDW}}bx^2 + B_2. \quad (44)$$

Solving for the constants with the boundary conditions specified above, we find

$$A = \frac{1 - \alpha - \beta}{J_{\text{DDW}}[8x_0 - 2x_0^2(a+b) - 12 + 2b] + 1},$$

$$B_1 = \alpha, B_2 = 1 - \beta - A(1 - 12J_{\text{DDW}} + 2J_{\text{DDW}}b) \quad (45)$$

We study two cases:

(a) $x_0 = 1/2$. We choose $a = b = 2$, giving

$$q(x) = \frac{1}{1+2x}, \quad 0 \leq x \leq \frac{1}{2},$$

$$= \frac{1}{3-2x}, \quad \frac{1}{2} \leq x \leq 1. \quad (46)$$

The equation for the coexistence line in the present case is obtained from (17) and reads

$$\alpha = \beta, \quad (47)$$

identical to that in a uniform open TASEP. Mean-field solution for $\rho_{\text{DDW}}(x)$ is then obtained from (45), which is shown in Fig. 10(top). The corresponding MCS results are also plotted, which agree well with the MFT solution, but clearly deviates from its counterpart in an open, uniform TASEP with $\alpha = 0.07, \beta = 0.07$. This deviation is due to the space dependence of $q(x)$. The local normalised probability distribution $P(x)$ [see Eq. (26)] and domain wall height $\Delta(x)$ [see Eq. (32)] in this case are shown in Fig. 10(bottom). Both are space dependent.

(b) Next we choose $x_0 = 1/3$. We choose $a = 4, b = 2$, giving

$$q(x) = \frac{1}{1+4x}, \quad 0 \leq x \leq \frac{1}{3},$$

$$= \frac{1}{3-2x}, \quad \frac{1}{3} \leq x \leq 1. \quad (48)$$

The equation for the coexistence line in the present case is obtained from (17) and reads

$$\alpha = \beta, \quad (49)$$

identical to that in a uniform open TASEP. Notice that the coexistence line (49) is identical to the previous case (47), *in spite of* having different $q(x)$ in these two cases. This is because, the coexistence line is controlled by the ratio of $q(0)$ and $q(1)$, which is unity in both these cases.

Mean-field solution for $\rho_{\text{DDW}}(x)$ is then obtained from (45), which is shown in Fig. 11. The corresponding MCS results are also plotted, which agree well with the MFT solution, but clearly deviates from its counterpart in an open, uniform TASEP with $\alpha = 0.07, \beta = 0.07$. This deviation is due to the space dependence of $q(x)$. The local normalised probability distribution $P(x)$ [see Eq. (26)] and domain wall height $\Delta(x)$ [see Eq. (32)] in this case are shown in Fig. 11(bottom). Both are space dependent.

(iv) Now we study the stationary densities with hopping rate functions $q(x)$ having a finite discontinuity at

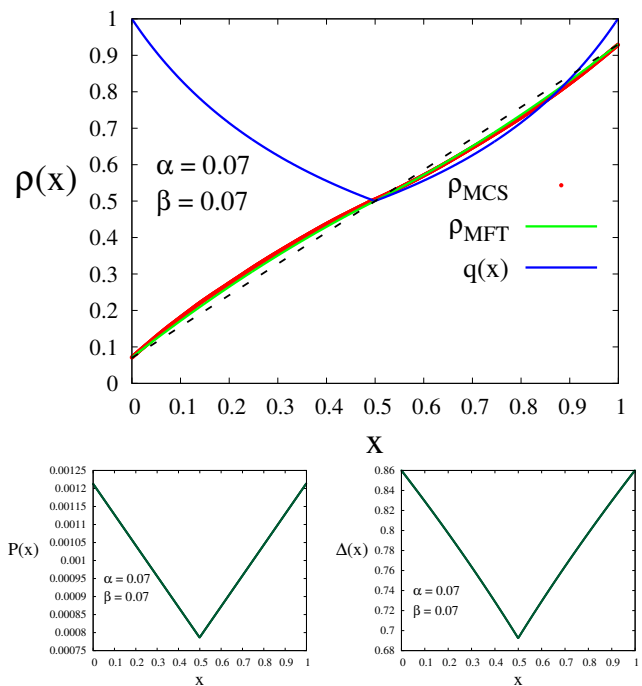


FIG. 10: (top) Density profile (43) for $\rho_{\text{DDW}}(x)$ on the coexistence line (47) with $q(x)$ as given in (46) and $\alpha = 0.07, \beta = 0.07$. Both MFT (green line) and MCS (red dots, system size $L = 1000$) are shown, which agree well with each other. The broken line is the reference line with $\alpha = 1 - \beta = 0.07$, which is the DDW envelop with $\alpha = 0.07, \beta = 0.07$ in an open, uniform TASEP. The deviation of $\rho_{\text{DDW}}(x)$ from the DDW in an open, uniform TASEP is clearly visible. (bottom) Plots of the corresponding local probability $P(x)$ (left) and domain wall height $\Delta(x)$ (right) are shown. Both are space dependent. See text.

$x = x_0$, in contrast to the previous cases where $q(x)$ is assumed to be continuous. Since the discontinuity of $q(x)$ is *finite*, from (29) $\rho_{\text{DDW}}(x)$ must also be continuous at $x = x_0$, the point of discontinuity of $q(x)$. Nonetheless, $d\rho_{\text{DDW}}/dx$ and hence probability $P(x)$ of finding the domain wall at x are *discontinuous* at $x = x_0$. Thus, $\rho_{\text{DDW}}(x)$ should have a kink at $x = x_0$. We study two distinct examples:

In the first case we choose

$$q(x) = \frac{1}{1+2x}, \quad 0 \leq x \leq \frac{1}{2},$$

$$= \frac{1}{2x}, \quad \frac{1}{2} \leq x \leq 1, \quad (50)$$

such that $q(x)$ is discontinuous at $x = 1/2$. The discontinuity is finite of size $1/2$. The equation for the coexistence line can be obtained from (17) and is given by (34), since $q(0) = 1, q(1) = 1/2$, same as for case (i) above. We thus see that the discontinuity in $q(x)$ has no effect on the equation of the coexistence line. However, the DDW profile $\rho_{\text{DDW}}(x)$ is affected by it, as we derive below.

We continue to use the general solution for $\rho_{\text{DDW}}(x)$

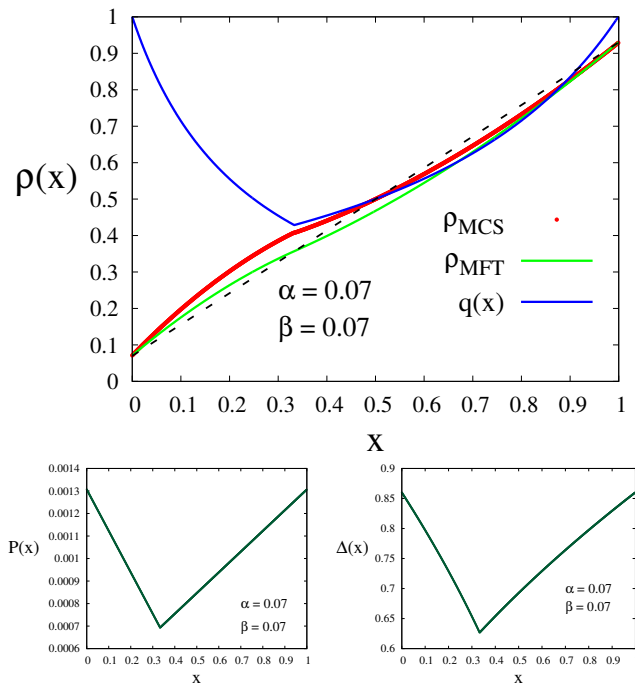


FIG. 11: (top) Density profile (43) for $\rho_{DDW}(x)$ on the coexistence line (49) with $q(x)$ as given in (48) and $\alpha = 0.07, \beta = 0.07$. Both MFT (green line) and MCS (red dots, system size $L = 1000$) are shown, which agree well with each other. The broken lines correspond to $\alpha = \beta = 0$. and $\alpha = \beta = 0.1$, which would have been the DDW profile in an open, uniform TASEP. (b) (bottom) Plots of the corresponding local probability $P(x)$ (left) and domain wall height $\Delta(x)$ (right) are shown. Both are space-dependent. see text.

as given in (43). We find

$$\begin{aligned} \rho_{DDW}(x) &= A[x - 4J_{DDW}x - 4J_{DDW}x^2] + B_1, \quad 0 \leq x \leq 1/2, \\ &= A[x - 4J_{DDW}x^2] + B_2, \quad 1/2 \leq x \leq 1, \end{aligned} \quad (51)$$

The coefficients A, B_1, B_2 are to be evaluated by using the boundary conditions (i) $\rho_{DDW}(x=0) = \alpha$, (ii) $\rho_{DDW}(x=1) = 1 - \beta$ and (iii) $\rho_{DDW}(x \rightarrow 1/2_-) = \rho_{DDW}(x \rightarrow 1/2_+)$. We find

$$\begin{aligned} B_1 &= \alpha, \\ B_2 &= \frac{1}{1 - 6J_{DDW}} \left[\alpha - 4\alpha J_{DDW} - 2J_{DDW} + 2J_{DDW}\beta \right], \\ A &= \frac{1 - \beta - B_2}{1 - 4J_{DDW}}, \end{aligned} \quad (52)$$

giving us $\rho_{DDW}(x)$ for a hopping rate function (50). We have shown plots of $\rho_{DDW}(x)$ versus x from our MFT prediction, superposed with the corresponding MCS result, in Fig. 12 (top). As expected and similar to the previous case, $\rho_{DDW}(x)$ is continuous but has a kink at $x = 1/2$, the location of the discontinuity of $q(x)$. This discontinuity is however visible in the discontinuities of $P(x)$

and $\Delta(x)$; see Fig. 12(bottom, left) and Fig. 12(bottom, right), respectively. Unsurprisingly, $\rho_{DDW}(x)$ clearly deviates from its counterparts in an open, uniform TASEP either with $\alpha = 0.1, \beta = 0.1$, or with $\alpha = 0.24, \beta = 0.24$. This deviation is due to the space dependence of $q(x)$. The local normalised probability distribution $P(x)$ [see Eq. (26)] and domain wall height $\Delta(x)$ [see Eq. (32)] in this case are shown in Fig. 10(bottom). Both are space dependent.

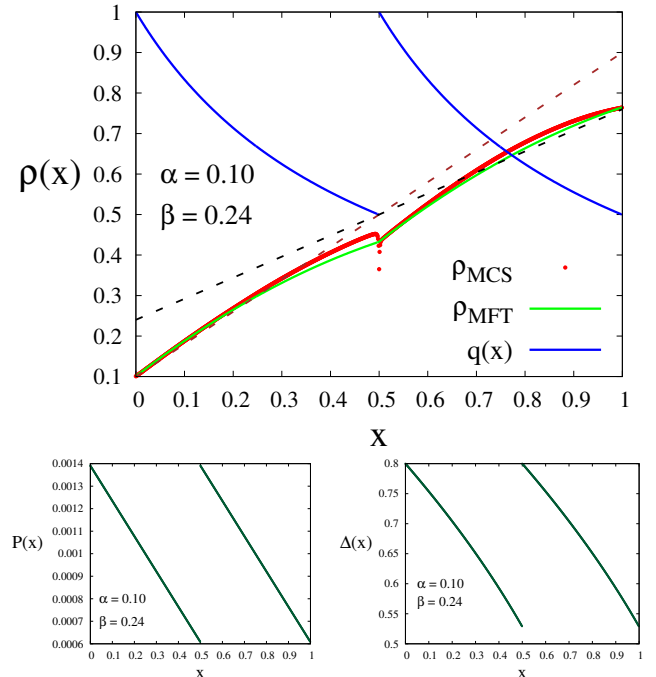


FIG. 12: (top) Density profile (43) with (52) for $\rho_{DDW}(x)$ on the coexistence line (34) with $q(x)$ as given in (50) and $\alpha = 0.1, \beta = 0.24$. Both MFT (green line) and MCS (red dots, system size $L = 1000$) are shown, which agree well with each other. The broken lines correspond to $\alpha = 0.1, \beta = 0.9$ and $\alpha = 0.24, \beta = 0.76$, which would have been the DDW profiles in an open, uniform TASEP with $\alpha = \beta = 0.1$ and $\alpha = \beta = 0.24$. (b) (bottom) Plots of the corresponding local probability $P(x)$ (left) and domain wall height $\Delta(x)$ (right) are shown. Both are space-dependent. See text.

Finally, we consider

$$\begin{aligned} q(x) &= \frac{1}{2 - 2x}, \quad 0 \leq x \leq \frac{1}{2}, \\ &= \frac{1}{3 - 2x}, \quad \frac{1}{2} \leq x \leq 1. \end{aligned} \quad (53)$$

The equation for the coexistence line can be obtained from (17) and is given by (39), since $q(0) = 1/2, q(1) = 1$, same as for case (ii) above. Nonetheless, $\rho_{DDW}(x)$ is affected by the specific form of $q(x)$ in (53) as we show below.

Using (43) together with (53), we get

$$\begin{aligned}\rho_{\text{DDW}}(x) &= A[x - 8J_{\text{DDW}}x + 4J_{\text{DDW}}x^2] + B_1, \quad 0 \leq x \leq \frac{1}{2}, \\ &= [x - 12J_{\text{DDW}}x + 4J_{\text{DDW}}x^2] + B_2.\end{aligned}\quad (54)$$

As before, the constants A, B_1, B_2 are to be evaluated by using the boundary conditions (i) $\rho_{\text{DDW}}(x=0) = \alpha$, (ii) $\rho_{\text{DDW}}(x=1) = 1 - \beta$ and (iii) $\rho_{\text{DDW}}(x \rightarrow 1/2_-) = \rho_{\text{DDW}}(x \rightarrow 1/2_+)$. We find

$$\begin{aligned}B_1 &= \alpha, \\ B_2 &= \alpha + \frac{9J_{\text{DDW}}}{2} \frac{1 - \beta - B_2}{1 - 8J_{\text{DDW}}}, \\ A &= \frac{1 - \beta - B_2}{1 - 8J_{\text{DDW}}},\end{aligned}\quad (55)$$

giving us $\rho_{\text{DDW}}(x)$ for a hopping rate function (50). We have shown plots of $\rho_{\text{DDW}}(x)$ versus x from our MFT prediction, superposed with the corresponding MCS result, in Fig. 13(top). As expected and similar to the previous case, $\rho_{\text{DDW}}(x)$ is continuous but has a kink at $x = 1/2$, the location of the discontinuity of $q(x)$. This discontinuity is however visible in the discontinuities of $P(x)$ and $\Delta(x)$; see Fig. 13(a) and Fig. 13(b), respectively. Unsurprisingly, $\rho_{\text{DDW}}(x)$ clearly deviates from its counterparts in an open, uniform TASEP either with $\alpha = 0.1, \beta = 0.1$, or with $\alpha = 0.24, \beta = 0.24$. This deviation is due to the space dependence of $q(x)$. The local normalised probability distribution $P(x)$ [see Eq. (26)] and domain wall height $\Delta(x)$ [see Eq. (32)] in this case are shown in Fig. 10(bottom). Both are space dependent.

V. PHASE TRANSITIONS AND UNIVERSAL PHASE DIAGRAMS

We now obtain the phase diagrams in the $\alpha - \beta$ plane for a few representative examples of $q(x)$. The different phase boundaries can be obtained by equating the corresponding stationary currents. Using the stationary currents in the LD, HD and MC phases, respectively, as defined in Eqs. (3)-(5), we obtain the general conditions for obtaining the phase boundaries as follows. The LD-MC phase boundary is given by

$$q(0)\alpha(1 - \alpha) = \frac{q_{\text{min}}}{4}.\quad (56)$$

The HD-MC phase boundary is given by

$$q(1)\beta(1 - \beta) = \frac{q_{\text{min}}}{4}.\quad (57)$$

Lastly, the LD-HD phase boundary is given by

$$q(0)\alpha(1 - \alpha) = q(1)\beta(1 - \beta),\quad (58)$$

which unsurprisingly is the line in the $\alpha - \beta$ plane on which a DDW is observed.

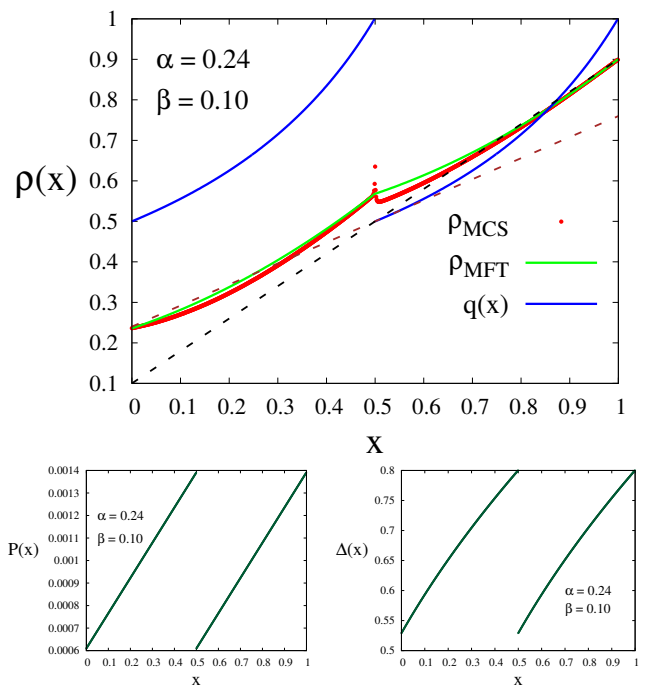


FIG. 13: (top) Density profile (43) with (55) for $\rho_{\text{DDW}}(x)$ on the coexistence line (39) with $q(x)$ as given in (50) and $\alpha = 0.1, \beta = 0.24$. Both MFT (green line) and MCS (red dots, system size $L = 1000$) are shown, which agree well with each other. The broken lines correspond to $\alpha = 0.1, \beta = 0.9$ and $\alpha = 0.24, \beta = 0.76$, which would have been the DDW profiles in an open, uniform TASEP with $\alpha = \beta = 0.1$ and $\alpha = \beta = 0.24$. (b) (bottom) Plots of the corresponding local probability $P(x)$ (left) and domain wall height $\Delta(x)$ (right) are shown. Both are space dependent. See text.

We now explicitly calculate the phase boundaries for some choices of $q(x)$.

(i) We begin with Case I above. With $q(x)$ as given in (10), we note that

$$q(0) = q_{\text{min}} = q(1) = \frac{3}{4}.\quad (59)$$

This gives

$$\alpha(1 - \alpha) = \frac{1}{4} \implies \alpha = \frac{1}{2}\quad (60)$$

as the LD-MC phase boundary. Similarly,

$$\beta(1 - \beta) = \frac{1}{4} \implies \beta = \frac{1}{2}\quad (61)$$

as the HD-MC phase boundary. Finally, we get

$$\alpha(1 - \alpha) = \beta(1 - \beta) \leq \frac{1}{4} \implies \alpha = \beta \leq \frac{1}{2}\quad (62)$$

is the phase boundary between the LD and HD phases. We thus find that the phase boundaries (60), (61) and

(62) are *identical* to their counterparts for a uniform open TASEP, with the phase boundaries meeting at $(1/2, 1/2)$; see Fig. 14. Thus the phase diagram in the $\alpha - \beta$ plane is identical with that for a uniform open TASEP. Thus calculation of the phase diagram *cannot* distinguish between a uniform open TASEP and an open TASEP with a hopping rate function given in (10). Are these two cases statistically identical then? We argue that this is not so. In fact, our Case I is fundamentally different from an open uniform TASEP. This is revealed in the nature of the respective phase transitions in the two models. In case of a uniform open TASEP, the LD-MC and HD-MC transitions are continuous transition [8, 43], since the LD phase bulk density α smoothly matches with the MC phase bulk density of $1/2$ at $\alpha = 1/2$. Similar considerations for the HD to MC transition show that it is also a continuous transition. In contrast, in Case I of our study, $\rho_{LD}(x) < 1/2$ *even* at the transition point to the MC phase with $J_{LD} = J_{MC}$, except at isolated points where $q(x) = q_{\min}$. This means the spatial average of the stationary LD phase density

$$\bar{\rho}_{LD}(x) \equiv \int_0^1 dx \rho_{LD}(x) < 1/2 = \bar{\rho}_{MC} \equiv \int_0^1 dx \rho_{MC}(x), \quad (63)$$

the mean density in the MC phase, even at the transition point, giving a *discontinuous transition*, in contrast to a uniform open TASEP; see also Refs. [41, 42] for detailed discussions. The jump in the mean densities across the LD-MC transition is given by

$$\Delta\rho_{LD-MC} = 2 \int_0^1 dx \sqrt{1 - \frac{q_{\min}}{q(x)}}. \quad (64)$$

Similar arguments as above give that the HD-MC transition is also a discontinuous transition: the spatial average of the HD phase density

$$\bar{\rho}_{HD} \equiv \int_0^1 dx \rho_{HD}(x) < 1/2 = \bar{\rho}_{MC}, \quad (65)$$

since $\rho_{HD}(x) > 1/2$ *even* at the transition point to the MC phase with $J_{HD} = J_{MC}$, except at isolated points where $q(x) = q_{\min}$. The jump in the mean densities across the LD-MC transition is given by

$$\Delta\rho_{HD-MC} = \frac{1}{2} \int_0^1 dx \sqrt{1 - \frac{q_{\min}}{q(x)}}, \quad (66)$$

which in this particular case is same as (64).

Lastly, the LD-HD transition remains a discontinuous transition, as in a uniform open TASEP. The jump in the mean densities across the LD-HD transition is given by

$$\Delta\rho_{LD-HD} = \int_0^1 dx \sqrt{1 - \frac{q_{\min}}{q(x)}} \quad (67)$$

which is twice that of (64). The specific relations between the density jumps across the phase boundaries as given in

(64)-(67) apply only in this case due to the result $\bar{\rho}_{MC} = 1/2$.

Thus all the three transitions are discontinuous transitions here. This means the meeting point of the three phase boundaries in the $\alpha - \beta$ plane is *not* a multicritical point, since none of the three transitions here involves any critical point! This has another implication. It means the domain wall height $\Delta(x)$ in general *does not* vanish at the common meeting point of the phase boundaries, except at isolated points where $q(x) = q_{\min}$ (in this case at $x = 1/2$). If we thus consider the spatial average of the domain wall height as a function of α, β , it remains positive definite in this case:

$$\bar{\Delta} \equiv \int_0^1 \Delta(x) dx = \int_0^1 dx \sqrt{1 - \frac{4J_{DDW}}{q(x)}} > 0 \quad (68)$$

using (32). In contrast, the domain wall height in a uniform open TASEP necessarily vanishes at the multicritical point $(1/2, 1/2)$ in the $\alpha - \beta$ plane.

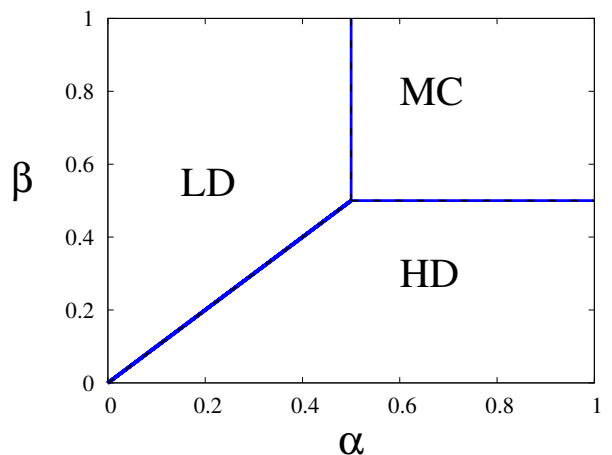


FIG. 14: Phase diagram in the $\alpha - \beta$ plane with $q(x)$ as given by (10) above. It is identical to the phase diagram for a uniform open TASEP. However, all the transitions are discontinuous in nature; see text.

(ii) We now construct the phase diagram for $q(x)$ in (13). In this case, $q_{\min} = 1/2, q(0) = 1, q(1) = 1/2$. This gives for the LD-MC phase boundary by using (56)

$$\alpha(1 - \alpha) = \frac{1}{8} \implies \alpha = \frac{1}{2} \left[1 - \frac{1}{\sqrt{2}} \right] < 1/2 \quad (69)$$

as the phase boundary between the LD and MC phases, which is *different* from a uniform open TASEP. In contrast, by using (57), we find

$$\beta(1 - \beta) = \frac{1}{4} \implies \beta = \frac{1}{2} \quad (70)$$

as the phase boundary between the HD and MC phases. This is unchanged from its uniform open TASEP result.

The LD-HD phase boundary is given by

$$\alpha(1-\alpha) = \frac{1}{2}\beta(1-\beta) \implies \beta = \frac{1}{2} \left[1 - \sqrt{1 - 8\alpha(1-\alpha)} \right], \quad (71)$$

which is a curved line, identical to the coexistence line on which a DDW can be found and clearly different from its counterpart in a uniform open TASEP. Phase boundaries (69), (70) and (71) meet at a common point $[(1-1/\sqrt{2})/2, 1/2]$, which is different from its counterpart in a uniform open TASEP.

See Fig. 15 for the phase diagram. While it has the same topology as the phase diagram in a uniform open TASEP, the LD-HD and LD-MC phase boundaries have shifted towards the β -axis, squeezing the LD phase area in the $\alpha-\beta$ plane. The HD-MC phase boundary remains at $\beta = 1/2$, but now extends to $[(1-1/\sqrt{2})/2, 1/2]$ towards the β -axis.

The LD to HD phase transition is as usual a discontinuous transition, marked by a finite density difference across the phase boundary. The LD to MC phase transition is also a discontinuous transition here for reasons similar to the discontinuous LD to MC phase transition with $q(x)$ in (10) as discussed above. Recall that in this case, $\rho_{MC}(x)$ is entirely given by $\rho_+(x) > 1/2$, with $J = J_{MC} = \frac{q_{\min}}{4}$, for all x . Furthermore, $\rho_{LD}(x) = \rho_-(x) < 1/2$ with $J = J_{LD} < J_{MC}$, for all x . This means $\bar{\rho}_{LD} < 1/2$ even at the threshold of the transition the MC phase, i.e., when $J_{LD} = J_{MC}$, whereas $\bar{\rho}_{MC} > 1/2$. The jump in the mean densities across the LD-MC phase boundary is again given by (64). In contrast, the transition between the HD and MC phases remains a continuous transition, as in a uniform open TASEP, albeit at a mean density different from $1/2$ at the transition point. This may be seen as follows. Noting that $\rho_{MC}(x)$ is entirely given by $\rho_+(x)$ with $J = q_{\min}/4$, $\rho_{HD}(x)$ smoothly matches with $\rho_{MC}(x)$ as $J_{HD} \rightarrow J_{MC}$. Naturally, at the threshold $\bar{\rho}_{HD} = \bar{\rho}_{MC}$, giving a continuous transition.

(iii) We now construct the phase diagram for $q(x)$ in (13). In this case, $q_{\min} = 1/2$, $q(0) = 1/2$, $q(1) = 1$. This gives for the LD-MC phase boundary by using (56)

$$\alpha(1-\alpha) = \frac{1}{4} \implies \alpha = \frac{1}{2} \quad (72)$$

as the phase boundary between the LD and MC phases. This is unchanged from its uniform open TASEP result. In contrast, by using (57), we find

$$\beta(1-\beta) = \frac{1}{8} \implies \beta = \frac{1}{2} \left[1 - \frac{1}{\sqrt{2}} \right] \quad (73)$$

as the phase boundary between the HD and MC phases. This is a curved line *different* from a uniform open TASEP. The LD-HD phase boundary is given by

$$\frac{1}{2}\alpha(1-\alpha) = \beta(1-\beta) \implies \alpha = \frac{1}{2} \left[1 - \sqrt{1 - 8\beta(1-\beta)} \right], \quad (74)$$

which is a curved line, identical to the coexistence line on which a DDW can be found and clearly different from its

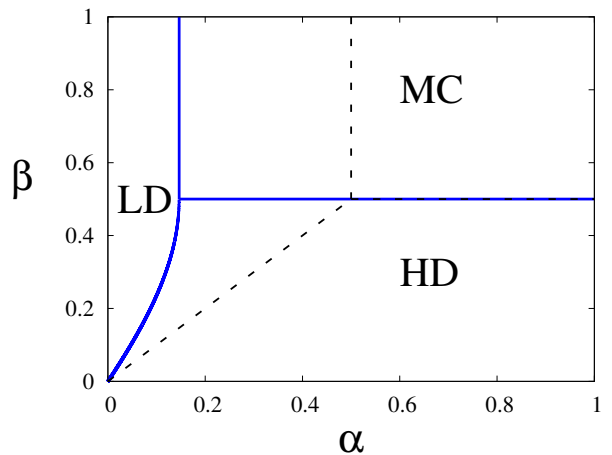


FIG. 15: Phase diagram in the $\alpha-\beta$ plane with $q(x)$ as given by (13) above. The phase diagram is different from but has the same topology as that in a uniform open TASEP. The broken lines give the LD-HD and LD-MC phase boundaries in an open, uniform TASEP as reference phase boundaries. The HD-MC phase boundary in the present case overlaps with that in an open, uniform TASEP. The LD-HD and LD-MC transitions are discontinuous, but the HD-MC transition is a continuous transition. See text.

counterpart in a uniform open TASEP. Phase boundaries (72), (73) and (74) meet at a common point $[1/2, (1-1/\sqrt{2})/2]$, which is different from its counterpart in a uniform open TASEP.

See Fig. 16 for the phase diagram. While it has the same topology as the phase diagram in a uniform open TASEP, the LD-HD and HD-MC phase boundaries have shifted towards the α -axis, squeezing the HD phase area in the $\alpha-\beta$ plane. The LD-MC phase boundary remains at $\alpha = 1/2$, but now extends to $[1/2, (1-1/\sqrt{2})/2]$ towards the α -axis.

The LD to HD phase transition is as usual a discontinuous transition, marked by a finite density difference across the phase boundary. The HD to MC phase transition is also a discontinuous transition here for reasons similar to the discontinuous HD to MC phase transition with $q(x)$ in (10) as discussed above. Recall that in this case, $\rho_{MC}(x)$ is entirely given by $\rho_-(x) < 1/2$, with $J = J_{MC} = \frac{q_{\min}}{4}$, for all x . Furthermore, $\rho_{HD}(x) = \rho_+(x) > 1/2$ with $J = J_{HD} < J_{MC}$, for all x . This means $\bar{\rho}_{HD} > 1/2$ even at the threshold of the transition the MC phase, i.e., when $J_{LD} = J_{MC}$, whereas $\bar{\rho}_{MC} < 1/2$. The jump in the mean densities across the HD-MC transition is given by (66) above.

In contrast, the transition between the LD and MC phases remains a continuous transition, same as in a uniform open TASEP (albeit at a mean density different from $1/2$ at the transition point). This may be seen as follows. Noting that $\rho_{MC}(x)$ is entirely given by $\rho_-(x)$ with $J = q_{\min}/4$, $\rho_{LD}(x)$ smoothly matches with $\rho_{MC}(x)$ as $J_{LD} \rightarrow J_{MC}$. Naturally, at the threshold $\bar{\rho}_{LD} = \bar{\rho}_{MC}$, giving a continuous transition. Notice the mutually com-

plementary picture of the phase diagram and the phase transitions between the last two cases. This is because the inherent complementary nature between the hopping rate function $q(x)$ in these two cases.

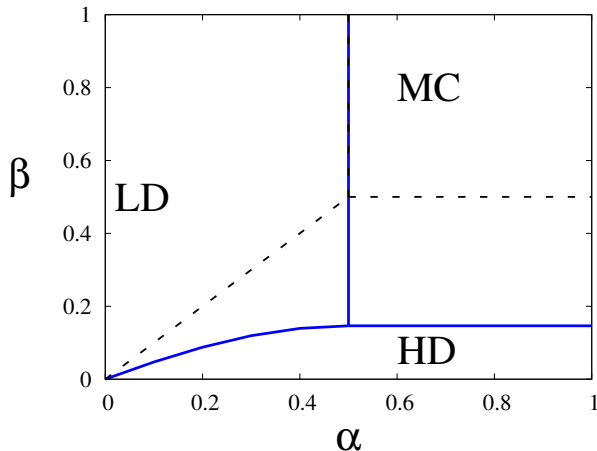


FIG. 16: Phase diagram in the $\alpha - \beta$ plane with $q(x)$ as given by (15) above. The phase diagram is different from but has the same topology as that in a uniform open TASEP. The broken lines give the LD-HD and HD-MC phase boundaries in an open, uniform TASEP as reference phase boundaries. The LD-MC phase boundary in the present case overlaps with that in an open, uniform TASEP. The LD-HD and HD-MC transitions are discontinuous, but the LD-MC transition is a continuous transition. See text.

A. Monte-Carlo simulations

Our model as defined in Section II above consists of a lattice of L sites, each of which is labelled by an index i with $i \in [1, L]$. We represent the occupation at site i at time t by $n_i(t)$, which is either 0 or 1. We perform MCS studies of the model subject to the update rules (a)-(c) described above in Sec. II by using a random sequential updating scheme. The particles enter the system through the left most site ($i = 1$) at a fixed rate α , a control parameter of the model, if it is vacant. Then after hopping through the system from $i = 1$ to L , subject to exclusion, the particles exit the system from $i = L$ at a fixed rate β , another control parameter of the model. Here, α and β are varied to produce different steady states. After reaching the steady states, the density profiles are calculated and temporal averages are performed. This produces time-averaged, space-dependent density profiles, given by $\langle n_i \rangle$, parametrised by α and β ; here $\langle \dots \rangle$ implies temporal averages over the steady states of the model. We have performed with $L = 10000$ ($L = 1000$ for the domain walls) up to 10^7 Monte-Carlo steps. The steady states are reached by the system after spending certain transient times. In an open TASEP,

the existence of a steady state is easily ascertained by observing the spatio-temporal constancy of the average density $\langle n_i(t) \rangle$ (excluding the domain walls) in the bulk of the system. In the present problem, this no longer holds due to the spatially varying steady state density in the bulk. Instead, we use the constancy of the current J in the steady state, a condition that holds both in the present study and also for a uniform open TASEP. In our MCS studies, all our measurements are done only after this condition is satisfied, i.e., a constant J is achieved.

VI. SUMMARY AND CONCLUSIONS

To summarise, we have studied the stationary densities and domain walls in open inhomogeneous TASEPs, characterised by hopping rates, which vary slowly in space. Building upon and extending the results in Ref. [42], we have obtained the stationary densities, which are generically space-dependent, and depend crucially on the precise space dependence of the hopping rate functions $q(x)$. For the particular choices of $q(x)$ made in the present study, we have shown that the steady state MC phase density $\rho_{MC}(x)$ can be discontinuous, even when $q(x)$ is *continuous*. We have shown how MFT arguments can be made in these cases, which are corroborated by our MCS simulations. We have studied the delocalised domain walls (DDW) in details and have calculated their envelopes analytically, which mark their departures from the DDWs in conventional open, uniform TASEPs. Furthermore, we have constructed the phase diagrams in the $\alpha - \beta$ plane, which reveal a remarkable degree of universality in their topology, independent of the forms of $q(x)$. In fact, in one case, the phase diagram matches *exactly* with that for an open, uniform TASEP. However, all the phase boundaries in the case represent discontinuous transitions. This shows the inadequacy of the phase diagrams as markers or proxies for $q(x)$. Even the knowledge of the phase transitions may not suffice. For instance, one can construct another $q(x)$ that has the same symmetry as in the case I in the Section Phase diagram, giving a phase diagram identical to that in an open, uniform TASEP and having all discontinuous transitions as in the case I. Thus, one needs to *actually* measure the full stationary densities to learn about the underlying $q(x)$. This is an important outcome from the present study.

Our studies here can be extended in a various directions. First of all, we have only concerned ourselves with studying the static or stationary properties. It will be interesting to explore how time-dependent properties can depend upon various $q(x)$. One can also study smoothly varying hopping rates in TASEP models connected to finite reservoirs and point defects. We hope our work here will provide impetus to future studies along these directions.

-
- [1] J. Ziman, *Models of Disorder: The Theoretical Physics of Homogeneously Disordered Systems*, Cambridge University Press, Cambridge, 1979.
- [2] R. Stinchcombe, Disorder in non-equilibrium models, *J. Phys.: Condens. Matter* **14**, 1473 (2002).
- [3] J. Krug, “Boundary-induced phase transitions in driven diffusive systems,” *Phys. Rev. Lett.* **67**, 1882 (1991).
- [4] B. Derrida, S. A. Janowsky, J. L. Lebowitz, and E. R. Speer, “Exact solution of the totally asymmetric simple exclusion process: Shock profiles,” *J Stat Phys*, 813–842.
- [5] B. Derrida and M. R. Evans, “Exact correlation functions in an asymmetric exclusion model with open boundaries,” *Journal de Physique I* **3**, 311 (1993).
- [6] B. Derrida, M. R. Evans, V. Hakim, and V. Pasquier, “Exact solution of a 1d asymmetric exclusion model using a matrix formulation,” *J. Phys. A: Math. and Gen.* **26**, computational biology 7, e1002203 (2011). 1493–1517 (1993).
- [7] C. T. MacDonald, J. H. Gibbs, and A. C. Pipkin, Kinetics of biopolymerization on nucleic acid templates, *Biopolymers* **6**, 1 (1968).
- [8] B. Derrida, An exactly soluble non-equilibrium system: The asymmetric simple exclusion process, *Phys. Rep.* **301**, 65 (1998).
- [9] A. Parmeggiani, T. Franosch, and E. Frey, Phase coexistence in driven one-dimensional transport, *Phys. Rev. Lett.* **90**, 086601 (2003).
- [10] A. Parmeggiani, T. Franosch, and E. Frey, Totally asymmetric simple exclusion process with Langmuir kinetics, *Phys. Rev. E* **70**, 046101 (2004).
- [11] T. Reichenbach, T. Franosch, and E. Frey, Exclusion processes with internal states, *Phys. Rev. Lett.* **97**, 050603 (2006).
- [12] T. Reichenbach, E. Frey, and T. Franosch, Traffic jams induced by rare switching events in two-lane transport, *New Journal of Physics* **9**, 159 (2007).
- [13] T. Reichenbach, T. Franosch, and E. Frey, Domain wall delocalisation, dynamics and fluctuations in an exclusion process with two internal states,” *Eur. Phys. J. E* **27**, 47 (2008).
- [14] T. Banerjee, A. K. Chandra, and A. Basu, Phase coexistence and particle nonconservation in a closed asymmetric exclusion process with inhomogeneities,” *Phys. Rev. E* **92**, 022121 (2015).
- [15] B. Daga, S. Mondal, A. K. Chandra, T. Banerjee, and A. Basu, Nonequilibrium steady states in a closed inhomogeneous asymmetric exclusion process with generic particle nonconservation,” *Phys. Rev. E* **95**, 012113 (2017).
- [16] I. R. Graf and E. Frey, Generic Transport Mechanisms for Molecular Traffic in Cellular Protrusions, *Phys. Rev. Lett.* **118**, 128101 (2017).
- [17] M. Bojer, I. R. Graf, and E. Frey, Self-organized system-size oscillation of a stochastic lattice-gas model, *Phys. Rev. E* **98**, 012410 (2018).
- [18] A. Goswami, U. Dey and S. Mukherjee, *Phys. Rev. E*
- [19] R. Lipowsky, S. Klumpp, and T. M. Nieuwenhuizen, Random walks of cytoskeletal motors in open and closed compartments, *Phys. Rev. Lett.* **87**, 108101 (2001).
- [20] S. Klumpp and R. Lipowsky, Traffic of molecular motors through tube-like compartments, *Journal of Statistical Physics* **113**, 233 (2003).
- [21] L.D. Fernandes and L. Ciandrini, Driven transport on a flexible polymer, *Phys. Rev. E* **99**, 052409 (2019).
- [22] O. Dauloudet *et al.*, Modelling the effect of ribosome mobility on the rate of protein synthesis, *Eur. Phys. J. E* **44**, 19 (2021).
- [23] Z. Cshaók and T. Vicsek, *J. Phys. A* **27**, L591 (1994).
- [24] J. Krug and P. Ferrari, Phase transitions in driven diffusive systems with random rates, *J. Phys. A* **29**, L465 (1994).
- [25] J. Krug, Phase separation in disordered exclusion models, *Braz. J. Phys.* **30**, 97 (2000).
- [26] S. A. Janowsky and J. L. Lebowitz, Finite-size effects and shock fluctuations in the asymmetric simple-exclusion process, *Phys. Rev. A* **45**, 618 (1992).
- [27] G. Tripathy and M. Barma, Driven lattice gases with quenched disorder: Exact results and different macroscopic regimes, *Phys. Rev. E* **58**, 1911 (1998).
- [28] N. Sarkar and A. Basu, Nonequilibrium steady-states in asymmetric exclusion processes on a ring with bottlenecks, *Phys. Rev. E* **90**, 022109 (2014).
- [29] T. Banerjee, N. Sarkar, and A. Basu, Generic nonequilibrium steady-states in an exclusion process on an inhomogeneous ring, *J. Stat. Mech. J. Stat. Mech.* P01024 (2015).
- [30] A. Haldar and A. Basu, Marching on a rugged landscape: Universality in disordered asymmetric exclusion processes, *Phys. Rev. Research* **2**, 043073 (2020).
- [31] A. Goswami, R. Chatterjee and S. Mukherjee, *cond-mat.stat-mech* Defect versus defect: stationary states of single file marching in periodic landscapes with road blocks, arXiv: 2402.08499 (2024).
- [32] T. Chou and G. Lakatos, Clustered Bottlenecks in mRNA Translation and Protein Synthesis, *Phys. Rev. Lett.* **93**, 198101 (2004).
- [33] J. J. Dong, B. Schmittmann and R. K. P. Zia, Towards a Model for Protein Production Rates, *J. Stat. Phys.* **128**, 21 (2007).
- [34] J. Keisers and J. Krug, Exclusion model of mRNA translation with collision-induced ribosome drop-off, *J. Phys. A: Math. Theor.* **56**, 385601 (2023).
- [35] C. Bao et al, Specific length and structure rather than high thermodynamic stability enable regulatory mRNA stem-loops to pause translation, *Nat. Comm.*, **13**, 988 (2022) [<https://doi.org/10.1038/s41467-022-28600-5>]
- [36] D. A. Phoenix and E. Korotkov, Evidence of rare codon clusters within Escherichia coli coding regions, *FEMS Microbiol. Lett.* **155**, 63 (1997).
- [37] W. L. Quek and L. Y. Chew, Mechanism of Traffic Jams at Speed Bottlenecks, **29**, 289 (2014). [<http://dx.doi.org/10.1016/j.procs.2014.05.026>]
- [38] R. J. Harris and R. B. Stinchcombe, *Phys. Rev. E* **70**, 016108 (2004)
- [39] G. Lakatos, J. O’Brien and T. Chou, Hydrodynamic mean-field solutions of 1D exclusion processes with spatially varying hopping rates, *Phys. A: Math. Gen.* **39**, 2253 (2006).
- [40] R. B. Stinchcombe and S. L. A. de Queiroz, Smoothly varying hopping rates in driven flow with exclusion, *Phys. Rev. E* **83**, 061113 (2011).
- [41] D. D. Erdmann-Pham, K. D. Duc, and Y. S. Song, The key parameters that govern translation efficiency, *Cell*

- systems **10**, 183 (2020).
- [42] A. Goswami, M. Chatterjee, and S. Mukherjee, Steady states and phase transitions in heterogeneous asymmetric exclusion processes, *J. Stat. Mech. - Th. Exp.* 123209 (2022).
- [43] R. A. Blythe and M. R. Evans, *J. Phys. A: Math. Theo.* **40**, R333 (2007).
- [44] N. Sarkar and A. Basu, *Phys. Rev. E* **90**, 022109 (2014).
- [45] T. Banerjee, A. K. Chandra, and A. Basu, *Phys. Rev. E* **92**, 022121 (2015).
- [46] A. Parmeggiani, T. Franosch, and E. Frey, *Phys. Rev. E* **70**, 046101 (2004).
- [47] T. Reichenbach, T. Franosch, and E. Frey, Traffic jams induced by rare switching events in two-lane transport, *Eur. Phys. J. E* **27**, 47 (2008).
- [48] T. Banerjee and A. Basu, Smooth or shock: Universality in closed inhomogeneous driven single file motions, *Phys. Rev. Research* **2**, 013025 (2020).
- [49] P. C. Hohenberg and B. I. Halperin, Theory of dynamic critical phenomena, *Rev. Mod. Phys.* **49**, 435 (1977).
- [50] B. Pal and A. K. Gupta, Exclusion process with scaled resources: Delocalized shocks and interplay of reservoirs, *Phys. Rev. E* **105**, 054103 (2022).